Communication

Not peer-reviewed version

Sediments as Sentinels of Pollution Episodes in the Middle Estuary of the Tinto River (SW Spain)

Luis Miguel Cáceres Puro , Francisco Ruiz * , Javier Bermejo Meléndez , Lucía Fernández Sutilo , Maria Luz González-Regalado Montero , Joaquín Rodríguez Vidal , Manuel Abad De los Santos , Tatiana Izquierdo Rebraca , Antonio Toscano Grande , Paula Gómez Gutiérrez , Verónica Romero Aguilar

Posted Date: 19 September 2023

doi: 10.20944/preprints202309.1210.v1

Keywords: sediment; pollution; core; geoaccumulation index; estuary; SW Spain

Communication

Sediments as Sentinels of Pollution Episodes in the Middle Estuary of the Tinto River (SW Spain)

Luis Miguel Cáceres [1], Francisco Ruiz [1,*], Javier Bermejo [2], Lucía Fernández [2], María Luz González-Regalado [1], Joaquín Rodríguez Vidal [1], Manuel Abad [3], Tatiana Izquierdo [3], Antonio Toscano [1], Paula Gómez [1] and Verónica Romero [1]

[1] Departamento de Ciencias de la Tierra, Universidad de Huelva, 21071-Huelva, Spain
[2] Departamento de Historia, Geografía y Antropología, Universidad de Huelva, 21071-Huelva, Spain
[3] Departamento de Biología y Geología, Física y Química Inorgánica, Universidad Rey Juan Carlos, 28933-Móstoles, Spain
* Correspondence: ruizmu@uhu.es

Abstract: Estuaries are excellent environments of identifying pollution episodes that have affected river basins, as their sediments are the final destination of some of the pollutants. This paper studies the geochemical evolution of five elements (As, Co, Cu, Pb, Zn) in a core extracted from the middle estuary of the Tinto River (SW Spain). Results are based on facies interpretation, ICP Atomic Emission Spectrometry analysis, the application of a regional background to obtain the geoaccumulation index and dating. Four pollution episodes have been detected at ~5.8 cal. kyr BP (acid mine drainage?), 4.7-4.5 kyr BP (first mining activities), the 1850-1960 interval (intensive mining) and the second half of the 20th century (intensive mining and industrial inputs). All episodes show an increase in one or more of these elements, as well as changes in their geochemical classes deduced from the geoaccumulation index.

Keywords: sediment; pollution; core; geoaccumulation index; estuary; SW Spain

1. Introduction

Numerous anthropogenic activities (e.g., industrial effluents, mining waste, agricultural residues, urban inputs), the natural erosion of geological formations or even high-energy events (river floods, storms, tsunamis, etc.) leave their mark on the geochemical levels of sediments and soils [1–6]. One of the most common effects is the increase in concentrations of certain elements, among which heavy metals are commonly used as a reference to measure the level of pollution [7–9]. To determine the heavy metal contamination in a soil or sediment, various indices are often used, such as the enrichment factor (EF) or the geoaccumulation index (I_{geo}), among others [10–13]. The latter index requires a regional background in order to calculate the degree of contamination, which may be unique for each metal regardless of grain size (e.g., [14,15]), or may include a differentiation between sandy and muddy sediments [16].

Estuaries are often the final repositories of many of these natural processes or human actions, as they often contain the inputs of heavy metals produced in their river basins at present or in the past [17–19]. In the last years, numerous investigations have focused on the historical heavy metal pollution of these environments, based on geochemical studies of continuous sediment cores [20–22]. Some of them have applied the geocumulation index to detect pollution episodes and, in conjunction with radiocarbon dating and historical data, to pinpoint the time interval in which they occurred [23,24].

The main objective of this short communication is the detection of natural or anthropogenic pollution episodes in a continuous sediment core extracted from the middle estuary of the Tinto River (SW Spain), based on the vertical geochemical variations and the application of the regional geoaccumulation index to five elements. The results obtained will be compared with previous palaeoenvironmental reconstructions and historical mining data to identify the age of these episodes and their importance according to the degree of contamination deduced.

Preprints (www.preprints.org) | NOT PEER-REVIEWED | Posted: 19 September 2023 doi:10.20944/preprints202309.1210.v1

2. Materials and Methods

2.1. Study area

The Tinto River is a small stream that flows through the southwest of Spain and forms a large estuary together with the Odiel river at its mouth in the Atlantic Ocean, surrounded by Neogene-Pleistocene formations (Figure 1A,B). The hydrodynamics of this estuary are tidally dominated, as river discharges are very rare and vary from minimum flows during very dry years to about 350 Hm^3 in rainy years [25]. The tidal regime is mesotidal (2.1 m), with a low diurnal inequality [26].

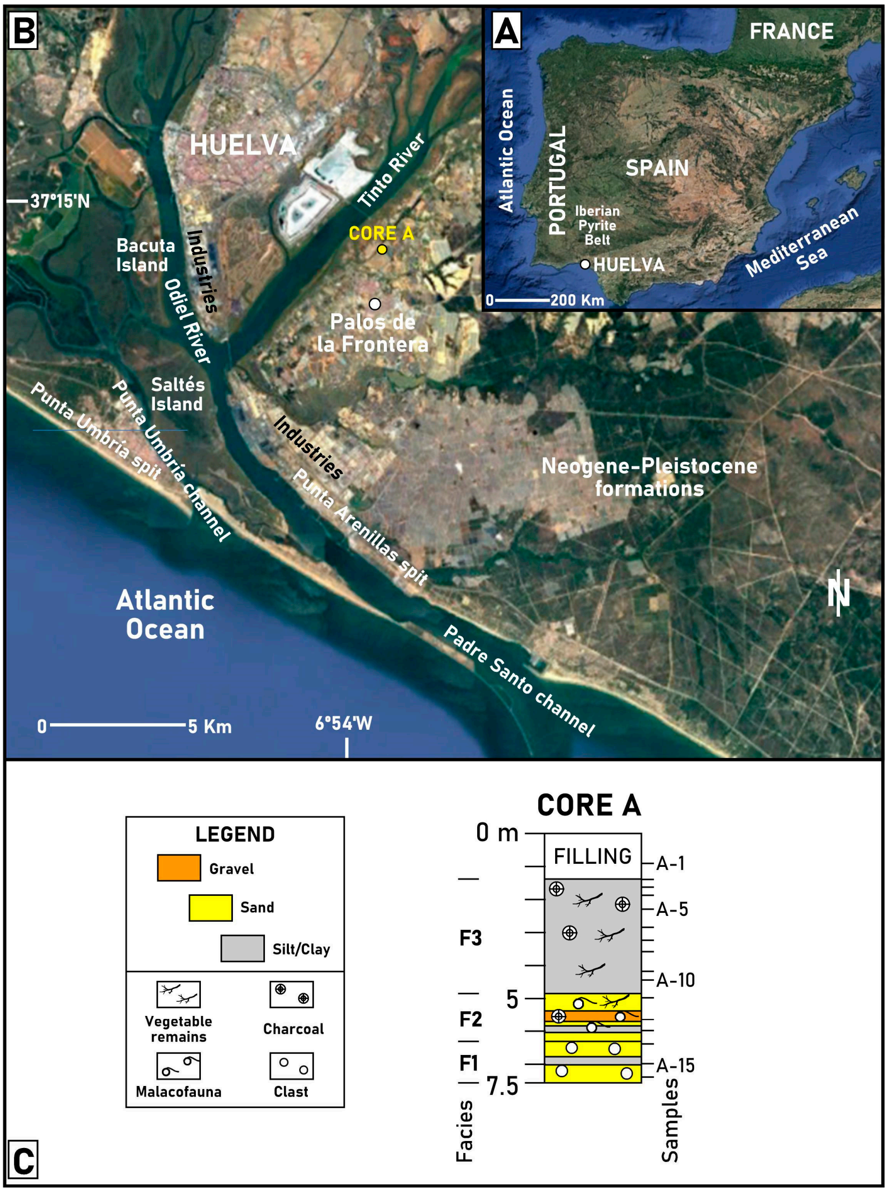

Figure 1. (A) Location of the Tinto-Odiel estuary. (B) Synthetic geomorphological map of the Tinto-Odiel estuary, with location of core A; (C) Log of core A, including sedimentary facies and sampling. (A)-(B): courtesy Google Earth.

This estuary can be divided into three sectors, depending on the interaction between river and tidal inputs [27]: i) fluvial estuary, composed of numerous braided channels; ii) middle estuary, with numerous marshes that come to form small islands (e.g., Figure 1B: Bacuta Island); and iii) marine estuary, with a central island (Figure 1B: Saltés Island), two main channels (Padre Santo channel, Punta Umbría channel) and two sandy spits (Punta Arenillas, Punta Umbría) that partially protect it.

In the marine estuary, wave energy is medium and 75% of the waves dot not exceed 0.5 m in height [28]. The coastal drift currents are oriented towards the east, with a high annual transport of sediment (1.8-3 x 10^5 m^3) [29,30] and have historically favoured the development of the two spits and the progressive closure of the innermost parts of the estuary.

2.2. Historical pollution

Southwest Spain is part of the Iberian Pyritic Belt, one of the most important metallogenic provinces in Europe, which includes some of the largest massive sulphide deposits in the world. These giant deposits have been exploited for 5,000 years within the Tinto River drainage basin [25], with an important mining activity during the Roman period (2100-1700 yr BP) and especially in the last 150 years, with an intensive extraction of pyrite and minor quantities of gold and silver. Currently, the waters of the Tinto River suffer from acid mine drainage, due to this age-old mining activity and to the heavy metal-rich inputs from the washing of the waste dumps generated [31].

In addition, this estuary has been affected by discharges from two industrial concentrations located on its banks since the 1960s (Figure 1B), made up of copper producers, fertiliser factories and refineries, among others. As a final result of these mining-industrial pollutant inputs, the surface sediments of the Tinto-Odiel estuary are among the most polluted in the world, with very high concentrations of As (up to 3,000 mg kg^{-1}), Cu (up to 4,415 mg kg^{-1}), Pb (up to 10,400 mg kg^{-1}) and Zn (up to 5,280 mg kg^{-1}) in its surface sediments [16,32]. Since 1985, this zone has come under a corrective plan for the control of industrial waste disposal.

2.3. Coring, sampling and Holocene palaeoenvironmental evolution

Core A (Figure 1B,C; 7.5 m depth; 37°14′06″N; 6°53′54″W) was extracted in the middle estuary of the Tinto River by usual rotary drilling techniques, with an almost continuous recovery of sediment and a barrel diameter of 11.6 mm. Sixteen samples (2 cm thickness) were obtained, with a distribution of samples linked to: a) the presence of different sedimentary facies; b) the definition of its limits; and c) the visual distribution of bioclasts in the core. The Holocene paleoenvironmental reconstruction of this core was inferred by [33], with basal alluvial sands (Figure 1C: facies F1), bioclastic sands and gravels from the marine flood of this area during the MIS-1 transgression (F2) and upper muddy marsh deposits (F3).

2.4. Chemical analysis

The chemical analysis of sixteen sediment samples were performed and certified by MS Analytical, Langley (Canada). Samples were collected manually by hand picking. They were respectively crushed and subsequently ground into powder using an agate mortar. The concentrations of five elements (As, Co, Cu, Pb, Zn) were obtained by ICP Atomic Emission Spectrometry (total digestion with concentrated acids), with less than 5% variation between different replicate samples and a quality control based on more than 30 references (e.g., OREAS 904). In these samples, detection limits vary between 0.01 mg kg^{-1} (e.g., Co) and 2 mg kg^{-1} (e.g., Zn).

2.5. Background and geoaccumulation index

A regional background of this estuary was obtained by [**34**] for both sandy and muddy sediments. This background was applied to obtain the geoaccumulation index of the extracted sediments, according to the following formula:

$$I_{geo} = \log_2 C_n/1.5 \times B_n,$$

where C_n is the concentration of an element in a given sample and B_n is the background of that element for the grain size of that sample (e.g., sand or mud). This background differentiates sandy (S) and muddy (M) sediments: As (S: 6.8 mg kg^{-1}; M: 7.3 mg kg^{-1}), Co (S: 4.2 mg kg^{-1}; M: 6.8 mg kg^{-1}), Cu (S: 13.1 mg kg^{-1}; M: 13 mg kg^{-1}), Pb (S: 4.3 mg kg^{-1}; M: 15.4 mg kg^{-1}) and Zn (S: 15.9 mg kg^{-1}; M: 39 mg kg^{-1}).

The pollution classes originally proposed by [35] have been slightly modified as follows: unpolluted (UP; $I_{geo} < 0$), very low polluted (VLP; $0 < I_{geo} < 1$), low polluted (LP; $1 < I_{geo} < 2$), moderately polluted (MP; $2 < I_{geo} < 3$), highly polluted (HP; $3 < I_{geo} < 4$), very highly polluted (VHP; $4 < I_{geo} < 5$) and strongly polluted (SP; $I_{geo} > 5$).

2.6. Dating

Two dates of core A were produced at the National Center of Accelerators (Sevilla, Spain). These dates were calibrated using CALIB version 8.2 and the final results correspond to calibrated ages using 2σ intervals.

3. Results and discussion

3.1. Facies, geochemistry and dating

The basal alluvial sandy-muddy deposits of this core (F1; 7.5-6.3 m depth; samples A-16 to A-14) have very low concentrations of most of the elements studied, even lower than the regional background (Table 1). They were deposited during the middle Holocene, according to the dating obtained near the boundary between F1 and F2 (Figure 1C and Table 2; sample A-13; ~5.8 cal. kyr BP). The bioclastic sediments of this last facies (6.3-4.9 m depth; samples A-13 to A-11; ~5.8-5 cal. kyr BP) were deposited during the flooding of this area due to the MIS-1 transgression. A first pollution level was detected near the base of this facies (sample A-13: ~5.8 cal. kyr BP) , with a noticiable increase in the concentrations of Cu (from 9.5 mg kg^{-1} to 39 mg kg^{-1}), Pb (from 11.1 mg kg^{-1} to 74.1 mg kg^{-1}) and Zn (from 25 mg kg^{-1} to 93 mg kg^{-1}). The age of this level would indicate an early natural pollution, as mining did not begin in this area until some thousand years later [25,36]. The origin of this first contamination is unknown, although it could come from a natural oxidation of the sulphides and formation of the gossans of the Iberian Pyritic Belt by acid rock drainage processes, which started more than 24 million years ago in this area [37]. Metals from the washing of these deposits would have been transported to the Tinto estuary and deposited in core A when its environment was flooded during the Holocene transgression.

The second pollution level was detected in the marshy muds collected near the base of F3 (Table 1: sample A-9), with some of the highest values of Cu (51.8 mg kg^{-1}), Pb (46.9 mg kg^{-1}) and Zn (107 mg kg^{-1}) of core A and increasing concentrations of As and Co. According to the average sedimentation rates (1.7-2 mm yr^{-1}) calculated by [38] in this estuary around 5000-4000 yr BP and the aforementioned dating, this new episode would have taken place approximately between ~4.7 kyr BP and ~4.5 kyr BP, coinciding with the development of the first mining and metallurgical works in this area [36].

Table 1. Geochemistry of core A (in mg kg^{-1}). Bold: three highest values of each element.

Sample	Depth (m)	Sediment	Facies	Interpretation	As	Co	Cu	Pb	Zn
A-1	0.9	Sand	Filling	Recent filling	7	3.7	21	14.7	30
A-2	1.4	Mud	F4	Marsh	**43.8**	**13.1**	**284.4**	**98**	**539**
A-3	1.6	Mud	F4	Marsh	**39.3**	**12.7**	27.5	37.9	88
A-4	1.9	Mud	F4	Marsh	**36.7**	**14.1**	23.8	23.2	85
A-5	2.3	Mud	F4	Marsh	18.3	12	20.3	22.1	87
A-6	2.8	Mud	F4	Marsh	19.2	12.1	22.7	27.9	89
A-7	3.3	Mud	F4	Marsh	17.2	10.3	15.7	40.6	68
A-8	3.6	Mud	F4	Marsh	22.2	11.5	22.8	18.6	87
A-9	4.2	Mud	F4	Marsh	30.1	12.4	**51.8**	**46.9**	**107**
A-10	4.5	Mud	F4	Marsh	18.2	9.7	18.5	17.8	69
A-11	5	Sand	F2	MIS-1 transgression	12.3	5.9	11.7	12.4	44
A-12	5.7	Gravel	F2	MIS-1 transgression	8.5	3.9	8.4	10	28

doi:10.20944/preprints202309.1210.v1

A-13	6	Mud	F2	MIS-1 transgression	27.3	10.6	**39**	**74.1**	**93**
A-14	6.4	Sand	F1	Alluvial	4.8	4.4	9.5	11.1	25
A-15	7	Mud	F1	Alluvial	6.7	6.4	10.9	14.9	33
A-16	7.4	Sand	F1	Alluvial	7.2	5.8	21.3	10.6	34

Table 2. Radiocarbon database.

Sample	Laboratory number	Material	$\delta^{13}C$ (%)	Uncalibrated age BP	Calibrated age BP	Mean Calibrated age (kyr BP)
A-12	CNA-4272	Organic matter	-22.6	6467±32	5483–5368	5.4
A-13	CNA-4274	Shell	-1.3	5428±33	5892–5711	5.8

The concentrations of the five elements decrease between 4.2 m depth and 2.3 m depth, with a further increase of As (from 18.3 mg kg^{-1} to 36.9-39.3 mg kg^{-1}) and, to a lesser extent, Pb (up to 37.9 mg kg^{-1}) observed between 1.9-1.6 m depth. This third pollution episode is associated with the start of intensive mining in the Tinto river basin from the second half of the 19th century to 1960. This increasing trend is confirmed at 1.4 m depth (e.g., the surface of core A before the recent antropic filling), with the maximum values of all five elements, and especially Cu (284.4 mg kg^{-1}), Pb (98 mg kg^{-1}) and Zn (539 mg kg^{-1}). This fourth episode would correspond to the conjunction of this intensive mining and inputs from nearby industrial complexes during the second half of the 20th century, which have caused a strong pollution in the recent sediments of the Tinto-Odiel estuary [39,40]. These high values confirm this last episode as the most important in the geochemical history of the middle estuary of the Tinto River. Transit to the overlying artificial filling is evidenced by the presence of unpolluted fine sands in the upper 1.3 m of this core (Table 1: sample A-1).

3.3. Geoaccumulation index and pollution episodes

These four episodes are also detected when I_{geo} is applied to the concentrations of the five elements (Figure 2). The first episode (~5.8 cal. kyr BP) is characterized by the transition from UP (As, Co, Cu) or VLP (Pb) sediments to VLP (Co) or LP (As, Cu, Pb) sediments. These four elements also show similar variations in their pollution class during the second episode (~4.7-4.5 kyr BP), most marked for Pb (from UP to LP) and to a lesser extent for As (from VLP to LP).

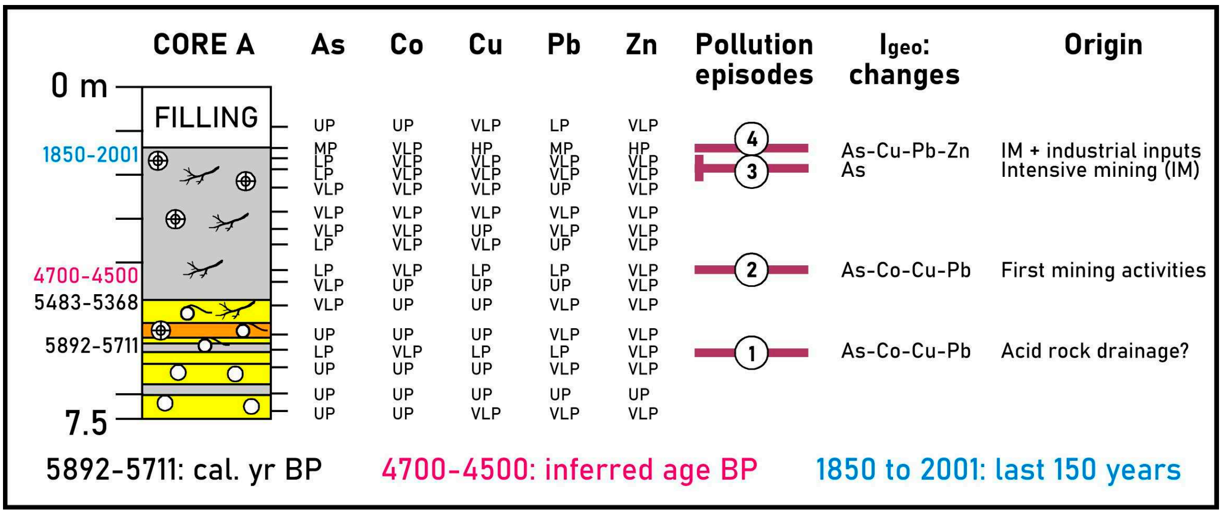

Figure 2. Application of I_{geo} to core A.

The third episode (~1850-1960) is mainly defined by As (from VLP to LP), although an increase in the concentration of most of the other elements is observed (see previous chapter). The fourth episode (~1960-2000) is clearly the most important, with the presence of MP (As, Pb) to HP (Cu, Zn)

Preprints (www.preprints.org) | NOT PEER-REVIEWED | Posted: 19 September 2023 doi:10.20944/preprints202309.1210.v1

sediments. Consequently, this last polluting episode is the most important in the geochemical history of the Tinto-Odiel estuary, as evidenced by the analysis of other sediment cores extracted in this area [34,41,42].

5. Conclusions

The joint application of geochemical analysis and the geoaccumulation index has proved to be an effective tool for detecting pollution episodes in the middle estuary of the Tinto River (SW Spain), in conjunction with historical data on mining activities in this area. Four episodes have been distinguished, characterised by an increase in the concentration of the elements studied and their geochemical classes based on I_{geo}. The first recorded pollution was of natural origin and coincided with the flooding of this estuary during the Holocene transgression. The next three episodes are linked to the start of mining activities, a period of intensive mining and the coincidence of intensive mining and the discharge of highly polluted industrial effluents into the estuary.

Author Contributions: All authors have participated in all stages of the paper.

Funding: This paper has been mainly financed by the Palos de la Frontera Council. It is also carried out through the following projects: a) DGYCIT project CTM2006-06722/MAR; b) DGYCIT project CGL2006-01412; c) Roman cities of the Baetica. CORPVS VRBIVM BAETICARVM (I) (CUB) (Andalusian Gouvernement); d) From the Atlantic to the Tyrrhenian. The Hispanic ports and their commercial relations with Ostia Antica. DEATLANTIR II - HAR2017-89154-P (Plan Nacional de I+D+i); and e) FEDER 2014-2020 project UHU-1260298. Other funds have come from Andalusian Government (groups HUM-132, RNM-238, and RNM-293). It is a contribution to the Research Center in Historical, Cultural and Natural Heritage (CIPHCN) of the University of Huelva.

Data Availability Statement: Data are available upon request to the corresponding author.

Conflicts of Interest: The authors declare no conflict of interest.

References

1. Chagué-Goff, C.; Szczucinski, W.; Shinozaki, T. Applications of geochemistry in tsunami research: A review. *Earth-Sci. Rev.* **2017**, *165*, 203-244. https://doi.org/10.1016/j.earscirev.2016.12.003.
2. Silva, H.F.; Silva, N.F.; Oliveira, C.M.; Matos, M.J. Heavy Metals Contamination of Urban Soils—A Decade Study in the City of Lisbon, Portugal. *Soil Syst.* **2021**, *5*, 27. https://doi.org/10.3390/soilsystems5020027.
3. Chebykina, E.; Abakumov, E.; Shamilishvilly, G.; Kouzov, S. Soil Diversity of the Island of Gogland in the Gulf of Finland: History of Land Development and Current Status. *Soil Syst.* **2022**, *6*, 85. https://doi.org/10.3390/soilsystems6040085.
4. Mangas-Suarez, M.; Garcia-Ordiales, E.; Pérez, J.A.; Álvarez, R.; Villa, A.; Ordoñez, A.; Roqueñí, N. Enrichment of Metals in the Sediments of an Industrially Impacted Estuary: Geochemistry, Dispersion and Environmental Considerations. *Appl. Sci.* **2022**, *12*, 10998. https://doi.org/10.3390/app122110998.
5. Papadimou, S.G.; Kantzou, O.-D.; Chartodiplomenou, M.-A.; Golia, E.E. Urban Soil Pollution by Heavy Metals: Effect of the Lockdown during the Period of COVID-19 on Pollutant Levels over a Five-Year Study. *Soil Syst.* **2023**, *7*, 28. https://doi.org/10.3390/soilsystems7010028.
6. Nassiri, O.; Rhoujjati, A.; Moreno-Jimenez, E., Hachimi, M.L.E.L. Environmental and Geochemical Characteristics of Heavy Metals in Soils Around the Former Mining Area of Zeïda (High Moulouya, Morocco). *Water Air Soil Pollut.* **2023**, *234*, 110. https://doi.org/10.1007/s11270-023-06103-3.
7. Niu, S.; Xia, Y., Yang, C., Liu, C. Impacts of the steel industry on sediment pollution by heavy metals in urban water system.
8. *Environ. Pollut.* **2023**, *335*, 122364. https://doi.org/10.1016/j.envpol.2023.122364.
9. Hossain, M.B.; Sultana, J.; Pingki, F.H.; Nur, A.; Mia, M.S.; Bakar, M.A.; Yu, J.; Paray, B.A.; Arai, T. Accumulation and contamination assessment of heavy metals in sediments of commercial aquaculture farms from a coastal area along the northern Bay of Bengal. *Front. Environ. Sci.***2023**, *11*, 1148360. https://doi.org/10.3389/fenvs.2023.1148360
10. Hamarashid, R.A.; Fiket, Ž.; Mohialdeen, I.M.J. Environmental Impact of Sulaimani Steel Plant (Kurdistan Region, Iraq) on Soil Geochemistry. *Soil Syst.* **2022**, *6*, 86. https://doi.org/10.3390/soilsystems6040086.
11. Kroeksakul, P.; Ngamniyom, A.; Silprasit, K.; Singhaboot, P. Relationship between Potential Trace Elements Contamination in Sediment and Macrofauna in the Upper Gulf of Thailand. *J. Environ. Public Health* **2023**, 4231930. https://doi.org/10.1155/2023/4231930.
12. Kumar, V.; Bhatti, R.C.; Kaur, R.; Singh, S.; Nirmala, C.; Singh, A.N. Comparative Geo-Accumulation Index Of Heavy Metal Concentration In The Urban Soils Of Chandigarh And Baddi Areas Under Industrial

Activities In A Lower Shiwalik Region, India. *Eur. Chem. Bull.* **2023**, *12*, 937-953. https://doi.org/10.48047/ecb/2023.12.si10.00110.
13. Fadlillah, L.N., Utami, S., Rachmawati, A.A.; Jayanto, G.D.; Widyastuti, M. Ecological risk and source identifications of heavy metals contamination in the water and surface sediments from anthropogenic impacts of urban river, Indonesia. *Heliyon* **2023**, *9*, e15485. https://doi.org/10.1016/j.heliyon.2023.e15485.
14. Hamarashid, R.A.; Fiket, Ž.; Mohialdeen, I.M.J. Environmental Impact of Sulaimani Steel Plant (Kurdistan Region, Iraq) on Soil Geochemistry. *Soil Syst.* **2022**, *6*, 86. https://doi.org/10.3390/soilsystems6040086.
15. Zaakour, F.; Kholaiq, M.; Khouchlaa, A.; El Mjiri, I.; Rahimi, A.; Saber, N. Assessment of Heavy Metal Contamination Using Pollution Index, Geo-Accumulation Index, and Potential Ecological Risk Index in Agricultural Soil – A Case Study in the Coastal Area of Doukkala (Morocco). *Ecol. Eng. Environ. Technol.* **2023**, *24*, 38–44. https://doi.org/10.12912/27197050/157037.
16. Kahangwa, C.A. Application of Principal Component Analysis, Cluster Analysis, Pollution Index and Geoaccumulation Index in Pollution Assessment with Heavy Metals from Gold Mining Operations, Tanzania. *J. Geosc. Environ. Protect.* **2022**, *10*, 303-317. https://doi.org/10.4236/gep.2022.104019.
17. Ruiz, F. Trace metals in estuarine sedirnents from the southwestern Spanish coast. *Mar. Poll. Bull.* **2001**, *42*, 481-489. https://doi.org/10.1016/S0025-326X(00)00192-2.
18. Li, H., Gu, Y., Liang, R., Wang, Y., Jordan, R.W., Wang, L., Jiang, S. Heavy metals in riverine/estuarine sediments from an aquaculture wetland in metropolitan areas, China: Characterization, bioavailability and probabilistic ecological risk. *Environ. Poll.* **2023**, *324*, 121370. https://doi.org/10.1016/j.envpol.2023.121370.
19. Chahouri, A., Lamine, I., Ouchene, H., Yacoubi, B., Moukrim, A., Banaoui, A. Assessment of heavy metal contamination and ecological risk in Morocco's marine and estuarine ecosystems through a combined analysis of surface sediment and bioindicator species: *Donax trunculus* and *Scrobicularia plana*. *Mar. Poll. Bull.* **2023**, *192*, 115076. https://doi.org/10.1016/j.marpolbul.2023.115076.
20. Wang, Q.; Huang, X.; Zhang, Y. Heavy Metals and Their Ecological Risk Assessment in Surface Sediments of the Changjiang River Estuary and Contiguous East China Sea. *Sustainability* **2023**, *15*, 4323. https://doi.org/10.3390/su15054323
21. Babasaheb, R.; Thorat, P.; Prasad, A.R. Heavy metal accumulation in a moderately polluted Ulhas estuary, Western India. *Reg. Stud. Mar. Sci.* **2023**, *60*, 102818. https://doi.org/10.1016/j.rsma.2023.102818.
22. Fan, J., Fan, D., Wu, Y. Spatiotemporal variations of heavy metal historical accumulation records and their influencing mechanisms in the Yangtze River Estuary. *Sci. Tot. Environ.* **2023**, *854*, 158733. https://doi.org/10.1016/j.scitotenv.2022.158733.
23. Filippi, G.; Dassenakis, M.; Paraskevopoulou, V.; Lazogiannis, K. Sediment quality assessment in an industrialized Greek coastal marine area (western Saronikos Gulf). *Biosgeosciences* **2023**, *20*, 163-189. https://doi.org/10.5194/bg-20-163-2023.
24. Ubonyaem, T.; Bureekul, S.; Charoenpong, C.; Luadnakrob, P.; Sompongchaiyakul, P. Preindustrial levels and temporal enrichment trends of mercury in sediment cores from the Gulf of Thailand. *Environ. Geochem. Health* **2023**, *45*, 4243-4256. https://doi.org/10.1007/s10653-022-01465-9.
25. Nishitha, D.; Amrish, V.N.; Arun, K.; Warrier, A.K.; Udayashankar, H.N.; Balakrishn, K. Study of trace metal contamination and ecological risk assessment in the sediments of a tropical river estuary, Southwestern India. *Environ. Monit. Assess*. **2022**, *194*, 94. https://doi.org/10.1007/s10661-021-09728-1.
26. Davis Jr., R.; Welty, A.; Borrego, J.; Morales, J.A.; Pendon, J.G.; Ryan, J.G. Rio Tinto estuary (Spain): 5000 years of pollution. *Environ. Geol*. **2000**, *39*, 1107–1116. https://doi.org/10.1007/s002549900096.
27. Borrego J.; Morales J.A.; Pendón J.G. Holocene flling of an estuarine lagoon along the mesotidal coast of Huelva: The Piedras River mouth, southwestern Spain. *J. Coast. Res*. **1993**, *9*, 242–254.
28. Borrego, J. Sedimentología del estuario del río Odiel (Huelva, S.O. España). Ph. D. Thesis, Universidad de Huelva, Huelva, Spain, 1992 (unpublished).
29. CEDEX (Centro de estudios y experimentación de Obras Públicas). *Dinámica litoral de la flecha de El Rompido (Huelva)*. Ministerio de Obras Públicas, Madrid, 1991; 100 p.
30. CEEPYC (Centro de Estudios y Experimentacion de Puertos y Costas 'Ramon Iribarren'). *Plan de estudio de la dinámica litoral de la Provincia de Huelva.* Informe Direccion General de Puertos y Costas, Madrid, 1979; 37 p.
31. Cuena, G.J. *Proyecto de regeneración de las playas de Isla Cristina. Informe del Servicio de Costas*. Ministerio de Obras Publicas y Turismo, Madrid, 1991, 100 p.
32. Olías, M.; Cánovas, C.R.; Macías, F.; Basallote, M.D.; Nieto, J.M. The evolution of pollutant concentrations in a river severely affected by acid mine drainage: Río Tinto (SW Spain). *Minerals* **2020**, *10*, 598. https://doi.org/10.3390/min10070598.
33. Nelson, C.H.; Lamothe, P.J. Heavy metal anomalies in the Tinto and Odiel River and estuary system, Spain. *Estuaries* **1993**, *16*, 496-511.
34. Arroyo, M.; Ruiz, F.; González-Regalado, M.L.; Rodríguez Vidal, J.; Cáceres, L.M.; Olías, M.; Campos, J.M.; Fernández, L.; Abad, M.; Izquierdo, T.; Gómez, P.; Toscano, A.; Romero, V.; Gómez, G. Natural and

anthropic pollution episodes during the Late Holocene evolution of the Tinto River estuary (SW Spain). *Sci. Mar*. **2021**, *85*, 113-123. https://orcid.org/0000-0002-6693-598X
35. Ruiz, F.; González-Regalado, M.; Borrego, J.; Morales, J.A.; Pendón, J.G., Muñoz, J.M. Stratigraphic sequence, elemental concentrations and heavy metal pollution in Holocene sediments from the Tinto-Odiel Estuary, southwestern Spain. *Environ. Geol.* **1998**, *34*, 270–278. https://doi.org/10.1007/s002540050278.
36. Muller, G. Index of Geoaccumulation in Sediments of the Rhine River. *J. Geol*. **1979**, *2*, 108-118.
37. Nocete, F. (2006). The first specialised copper industry in the Iberian peninsula: Cabezo Juré (2900-2200 BC). *Antiquity* **2006**, *80*, 646-657. https://doi.org/10.1017/S0003598X00094102.
38. Essalhi, M.; Sizaret, S.; Barbanson, L.; Chen, Y.; Lagroix, F.; Demory, F.; Nieto, J.M.; Sáez, R.; Capitán, M.A. A case study of the internal structures of gossans and weathering processes in the Iberian Pyrite Belt using magnetic fabrics and paleomagnetic dating. *Mineralium Deposita* **2011**, *46*, 981-999. https://doi.org/10.1007/s00126-011-0361-8.
39. Lario, J.; Zazo, C.; Goy, J.L.; Dabrio, C.J.; Borja, F.; Silva, P.G.; Sierro, F.; González, A.; Soler, V.; Yll, E. Changes in sedimentation trends in SW Iberia Holocene estuaries (Spain). *Quat. Int.* **2002**, *93-94*, 171-176. https://doi.org/10.1016/S1040-6182(02)00015-0.
40. Cabrera, F.; Conde, B.; Flores, V. Heavy metals in the surface sediments of the tidal river Tinto (SW Spain). *Fresen. Environ. Bull.* **1992**, *1*, 400-405. https://hdl.handle.net/11441/134478.
41. López-González, N.; Borrego, J.; Carro, B.; Soria-Lozano, O. Biodisponibilidad de Fe y metales pesados en los sedimentos de la ría de Huelva. *Geogaceta* **2005**, *37*, 219-222.
42. Ruiz, F.; Borrego, J.; González-Regalado, M.L.; López González, N.; Carro, B.; Abad, M. Impact of millennial mining activities on sediments and microfauna of the Tinto River estuary (SW Spain). *Mar. Poll. Bull.* **2008**, *56*, 1258-1264. https://doi.org/10.1016/j.marpolbul.2008.04.036.
43. Abad, M.; Arroyo, M.; Ruiz, F.; González-Regalado, M.L., Rodríguez Vidal, J.; Cáceres, L.M.; Toscano, A.; Gómez, P.; Gomez, G.; Romero, V. Miocene-Holocene paleoenvironmental changes in the Tinto River estuary (SW Spain) evidenced by sedimentology, geochemistry and fauna. *Carnets Geol.* **2022**, *22*, 825-845. https://hdl.handle.net/10.2110/carnets.2022.2219.